

Interdecadal Variations of Persistent Extreme Heat Events in Eastern China Under Global Warming

Naihui Zang (✉ zangnh18@lzu.edu.cn)

Lanzhou University

Junhu Zhao

Laboratory for Climate Studies, National Climate Center, China Meteorological Administration

Pengcheng Yan

Key Laboratory of Arid Climatic Change and Reducing Disaster of Gansu Province / Key Open Laboratory of Arid Climatic Change and Reducing Disaster of China Meteorological Administration, Institute of Arid Meteorology

Han Zhang

Lanzhou University

Shankai Tang

Lanzhou University

Feng Guolin

Lanzhou University

Research Article

Keywords: Interdecadal variations, global warming, PEHEs

Posted Date: June 10th, 2021

DOI: <https://doi.org/10.21203/rs.3.rs-565992/v1>

License:  This work is licensed under a Creative Commons Attribution 4.0 International License.

[Read Full License](#)

Version of Record: A version of this preprint was published at Theoretical and Applied Climatology on August 8th, 2021. See the published version at <https://doi.org/10.1007/s00704-021-03723-9>.

Abstract

Persistent extreme heat events (PEHEs) exert a more negative impact on society, including agriculture, plant phenology, power production and human health, compared to general EHEs. The temporal and spatial characteristics of summer PEHEs in eastern China were analysed based on a daily maximum temperature dataset from 759 stations over the period of 1961–2018. The results show the following: Persistent distributions of PEHEs show that they are characterized by an exponential decay with a drop in the decay rate. In terms of spatial distribution, there is an apparent regional difference in the duration of PEHEs. North China is dominated by multi-frequency and short-duration EHEs, while South China is the opposite. PEHEs in North China and the Huanghuai region mainly occur in June–July but mostly in July and August in South China. Strongly responding to global warming, the frequency and duration of PEHEs in North China have increased since the 1990s. However, the frequency of PEHEs in North China and the Huanghuai region has shown opposite trends in June–July since the beginning of the 21st century. Affected by the atmospheric circulations, the regional differences in PEHE frequency are also apparent. Since the beginning of the 21st century, the PEHEs in North China and the Huanghuai area have shown an increasing trend in August. The short-term PEHEs in the middle and lower reaches of the Yangtze River and South China increased rapidly in the 2000s, while long-term PEHEs increased in the 2010s. This study implies that attention should be paid to not only the frequency of EH days but also to the persistence of EHE which is a key characteristic of damaging EH.

1. Introduction

According to the special report on climate change from the Intergovernmental Panel on Climate Change, human-induced warming is approximately 1.0°C ($\pm 0.2^{\circ}\text{C}$) above pre-industrial levels, increasing at 0.2°C ($\pm 0.1^{\circ}\text{C}$) per decade (Allen et al. 2018). Against the backdrop of anthropogenic climate change, the frequency, intensity, and range of extreme heat events (EHEs) show a robust increasing trend on a global scale (Luterbacher et al. 2004; Vincent and Mekis 2006; Fischer and Knutti 2015; Karmalkar and Bradley 2017; Lu et al. 2018). The rate of temperature increase in Europe, Australia, and most parts of Asia is significantly higher than the global average, and the increasing trend of EHEs is even higher (Stocker 2014). The recorded warming in China since the early 1960s is almost twice as high as the global mean and approximately one-third higher than the global land average temperature trend (Sun et al. 2016).

Since the beginning of the 21st century, the losses and problems caused to human society by frequent persistent extreme heat events (PEHEs) have become increasingly severe. For instance, the PEHEs that swept Europe in the summer of 2003 caused 35,000 deaths (Luterbacher et al. 2004; Robine et al. 2008; Dole et al. 2011). In the summers of 2011 and 2012, severe PEHEs occurred in the United States (Hoerling et al. 2013; Ye et al. 2013). In the summer of 2017, PEHEs swept across North America, Europe, and Asia and triggered forest fires in the Russian Far East, western United States, and other regions (Wang et al. 2018). PEHE weather also occurred in southern China (for example, the weather event that lasted more than 35 days from June 30 to August 3, 2003) (Ye et al. 2013). The frequency of PEHEs in China has gradually increased (Qiao et al. 2018). In 2006, extremely rare high temperatures and droughts occurred

in southwestern China, and the duration of high temperatures at some sites lasted more than 50 days (Peng et al. 2007). In 2013, large-scale PEHEs occurred in South China, and the highest temperature in many places continuously broke historical records. The duration of this event (from June 28 to August 22, lasting 56 days) is also historically rare (Sun et al. 2014; Peng et al. 2016; Yang and Feng 2016). In the summer of 2017, central and eastern China suffered a large-scale PEHE impact (Wang et al. 2018). In the summer of 2018, the number of high-temperature days and the average maximum temperature at most sites in North China and Northeast China exceeded historical records (XU et al. 2019; Ren et al. 2020). Long-duration PEHEs have caused considerable losses to agricultural production and economic development in certain countries. According to statistics, direct financial losses in China due to meteorological disasters are approximately 200 billion per year, most of which can be attributed to extreme weather (Sun et al. 2011). This number has increased by 60% from 2015 to 2019 to more than 320 billion. At the same time, the impact region of extreme high-temperature events in China has also increased from 12–43% of the country's land area (Qin et al. 2015).

Both the difference in the duration and the scope of occurrence of PEHEs further result in a significant impact of differences. The damage caused by large-scale and long-lasting PEHEs is higher than that of small-scale and short-duration PEHEs. Most studies on the duration of extreme events have defined a threshold (LU et al. 2020; Zhou et al. 2020). For example, Wang et al. (2013) and Wang et al. (2018) defined EHEs lasting more than 5 days as PEHEs. Ye et al. (2013) defined EHEs lasting more than 6 days as PEHEs. Jia and Hu (2017) defined PEHEs with durations longer than 3 d, 5 d, and 7 d as weak, moderate, and strong heatwaves, respectively. The selection of the threshold of the PEHE duration is subjective without taking into account regional differences. Pfliegerer and Coumou (2018) defined a persistent event as the duration of a warm or cold day. Their study showed that persistence in summer has increased over the past 60 years in the Northern Hemisphere. Furthermore, the changes are particularly pronounced for prolonged events, suggesting a lengthening in the duration of heat waves. The above studies show that the threat of PEHEs to the economic development of eastern China will become increasingly serious.

There are considerable differences resulting in the differences in PEHE between regions (Meehl and Tebaldi 2004; Pfliegerer and Coumou 2018). PEHEs are associated with a persistent anticyclonic anomaly (Zhang et al. 2003; Meehl and Tebaldi 2004; WEI and SUN 2007). Eastern China is broad, and the circulations of different scales work together in this region. The substantial differences in the residence time of anticyclones result in different durations of PEHEs (Yuan et al. 2018). June-August is the main season for PEHEs, but research shows that PEHEs in other months also have a significant increasing trend. Our previous study found that EHEs in eastern China show obvious intraseasonal characteristics (Zang et al. 2019). The EHEs mainly occur in the Huanghuai region (the area between the lower Yellow River and the Huai River) in June and primarily occur in the Jiangnan to Jianghuai region from July to August. This is mainly related to the spatial progression of the East Asian summer monsoon. The study also found that since 2010, the frequency and intensity of EHEs decreased in early summer, while the opposite occurred in midsummer.

Based on this, this article conducts a systematic analysis of PEHEs in eastern China and performs a detailed analysis of the regional characteristics, intraseasonal differences, and interdecadal variations of PEHEs of different durations to explore the response of PEHEs to global warming, striving for a deeper understanding of the changing characteristics of PEHEs.

2. Data And Methods

2.1 Data

In this study, observed daily surface air temperature data from 1st January 1951 to 31st August 2018 for 2374 stations in China were provided by the National Weather Information Center of the China Meteorological Administration. To ensure the completeness and continuity of the time series, stations with the highest temperature (T_{\max}) missing for more than one day were excluded. Finally, T_{\max} data from the May–September period for 759 sites (Fig. 1a) in eastern China from 1961 to 2018 were used.

To analyse the associated circulation anomalies, the data sets of the NCEP-NCAR Reanalysis were used (Kalnay et al. 1996). The variables from the NCEP-NCAR Reanalysis include geopotential height, uwind at multiple pressure levels, with a horizontal resolution of $2.5^\circ \times 2.5^\circ$ during January 1979 to present.

2.2 Methods.

An EH day is an effective indicator of EH events, and the Chinese Meteorological Department defines 35°C as the EH threshold. An EH day is determined to have occurred when the maximum temperature of the day is higher than or equal to 35°C (Shi et al. 2009; Ding et al. 2010; Sun et al. 2011; Hong et al. 2020). In a previous study, we selected 35°C as a fixed threshold to analyse the frequency and intensity of summer EHEs in China and found that there are apparent interdecadal variations in EHEs in eastern China. Therefore, this paper still uses this fixed threshold to calculate the EHE days in early summer and midsummer first and then uses the empirical orthogonal decomposition (EOF) method to analyse the main modes and the corresponding time coefficients in eastern China to divide the subregion. Furthermore, according to the temperature series in different regions, the percentile threshold method is used to determine the EHE thresholds. The T_{\max} series of climatological summer for sites divided in the same region from 1961 to 2018 is computed, and then the top 10% high-temperature days are defined as the regional EH day to study the regional and seasonal differences in PEHEs (Huang et al. 1993; Min et al. 2013; Chen and Lu 2015; Wang et al. 2020).

3. Regional Variations Of Pehes In Eastern China

3.1 Temporal and spatial characteristics of EHEs

Affected by Jianghuai Meiyu and other factors, the spatial distribution of EHE days in eastern China has visible intraseasonal changes (Yuan et al. 2018; Zang et al. 2019). EHEs in early summer (June) mainly occur in the Huanghuai area and south of the Yangtze River. EHEs arise less frequently in the Jianghuai

area, so the spatial distribution in the eastern region is inconsistent. In midsummer (July and August), the area from South China to the Jianghuai region is affected by the West Pacific subtropical high, which increases and stretches westward, leading to an increase in the number of EHEs in the Yangtze River Basin (Peng et al. 2016). To further analyse the variations in PEHEs in eastern China, EOF of the anomalies of EHE days in early summer and midsummer from 1961 to 2018 was carried out to study both the spatial distribution and intraseasonal variation characteristics.

Figure 1 shows the spatial patterns of the first two leading EOF modes that analyse the EH day anomalies from 1961 to 2018, both in early summer and midsummer. The EOF1 of EH day anomalies in early summer (Fig. 1b) is characterized by warming in the Yellow–Huai River basin. The warm centre is located in the Huanghuai region. EOF2 features a north–south dipole in EH day anomalies over eastern China (Fig. 1c). The warm centre is located in southern China. The Huanghuai region has negative values. The spatial characteristics of the first leading mode of the EH day anomaly in midsummer (Fig. 1d) are obviously different from those in early summer. Compared with early summer, the positive centre of the first leading mode moved from the Huanghuai region to the middle and lower reaches of the Yangtze River. In midsummer, the second leading mode shows that the EH day anomaly over South China is opposite to that over Huanghuai basins (Fig. 1e). To explore the differences in PEHEs in eastern China, we divided all the stations in eastern China into four subregions for comparison according to the EOF results of the anomalies of EH days in early summer and midsummer.

1. South China (SC) includes stations within 22°-28°N,110°-123°E.
2. The Yangtze River valley (YRV) includes stations within 28°-33°N,110°-123°E.
3. The Huanghuai region (HHV) includes stations within 33°-38°N,110°-123°E.
4. North China (NC) includes stations within 38°-43°N,110°-120°E.

In previous studies, the eastern coastal areas of China were often divided into South China, the Yangtze River valley, and North China based on the overall climate characteristics of the local area (Chen and Lu 2015; Tang et al. 2020). According to the spatial characteristics of the EOF of the anomaly of the number of EH days, this paper divides the area north of the Yangtze River into the Huanghuai region and North China, which can better reflect the regional and seasonal differences of PEHEs.

Previous studies have shown that there are apparent early onset phenomena of EHEs in eastern China, especially in the past 10 years, and the range and intensity of EH days in May have increased significantly (Zang et al. 2019; LU et al. 2020, Wang et al. 2021). Therefore, this paper analyses the average frequency of EHEs per station in four subregions from May to September since 1961 (Fig. 2). Figure 2 shows that the frequency of EHEs in eastern China declined from the end of the 1960s, and the decline in the HHV was relatively large. In the 1980s, the frequency of EHEs in the HHV and YRV reached a minimum. The four regions showed an increasing trend in the late 1980s. In the 1990s, the frequency of EHEs in the eastern region began to increase gradually, and the increase in North China was the most significant.

There are obvious differences in the frequency and duration of EHEs in eastern China. In NC and HHV, EHEs occur 4.8 times per year on average at each site. However, in the YRV and SC, the average EHE occurrence per site is only 3.5 times per year. That is, the frequency of EHE occurrence in the northern region is higher than that in the southern region (Sun et al. 2011). For PEHEs that lasted more than 3 days, there was no significant difference in the average frequency of the 4 regions (0.91 (NC), 1.16 (HHV), 1.06 (YRV), 1.01 (SC), respectively). Although the frequency of EHEs in the north is more frequent than that in the south, the number of days and the overall duration of EHEs in the north are lower than those in the south. This shows that the main manifestation of the difference in EHEs in various regions of eastern China is the difference in the frequency distribution of PEHEs that last less than 3 days. The article will conduct a specific analysis in the next section.

In addition, most of the EHEs that occurred in the northern region began to increase in May of the 21st century and are EHEs lasting 1–2 days. Due to the lack of long-term PEHE event formation conditions (Pfleiderer and Coumou 2018), EHEs persisting for more than 3 days are less frequent. For the same reason, in the southern region, in September, except for a small number of EHEs lasting 1–2 days, EHEs lasting more than 3 days are rare. Therefore, the current May and September EHEs have smaller impact on PEHEs in eastern China than June-August, and subsequent studies mainly focus on EHEs in summer (June-August).

3.2 The interdecadal variations of PEHEs

To analyze the variations of PEHEs lasting 3 or more days between different regions, the duration of the EHEs at each site is determined separately. Figure 3 shows the annual average of EHE duration-frequency curve of a single station in four regions of eastern China. In the beginning, the frequency value of PEHEs in four regions is at the peak. Then, the frequency decays exponentially as the corresponding duration increases. Pfleiderer and Coumou (2018) also found similar attenuation characteristics when they studied the changes in persistent temperature events in the Northern Hemisphere land area. The relationship between the duration and frequency of different regions is quite different, which is related to the differences in the formation mechanism of PEHEs in eastern China (Zhang et al. 2003; Sun et al. 2011; Yuan et al. 2018).

The frequency of PEHEs that last from 3 to 6 days (short-term PEHEs) has the fastest attenuation rate, and the attenuation amplitude is higher than 60%. In this range, the attenuation amplitude of the PEHE frequency in the HHV was the largest, and in the 1960s, the attenuation amplitude of the PEHE frequency in the HHV exceeded 85%.

The frequency of short-term PEHEs in each region generally showed the characteristics of decadal variations that first decreased and then increased. Since the 1960s, the PEHE frequency began to decline until it reached a minimum in the 1980s and then began to increase. The frequency of PEHEs that occurred in the 2010s reached the maximum. The interdecadal variations in PEHE frequency in eastern China are consistent with those in EHE frequency (Wang et al. 2013; Zang et al. 2019). The decadal trends of short-term PEHE frequency in the YRV and SC are the same as those in NC and HHV. However,

the frequency of short-term PEHEs in the YRV and SC since the beginning of the 21st century is significantly higher than in the previous stage. In the 2000s especially, the frequency of short-term PEHEs even exceeded that of the 2010s. The frequency of PEHEs lasting more than 3 days in the four regions is roughly the same. The frequency of short-term PEHEs in NC and HHV in each decade is the same as that of YRV and SC, indicating that the difference in the number of EHE days in the eastern region is related to the long-term PEHE frequency.

In the four regions of eastern China, the frequency of PEHEs lasting 7 days or longer per year (long-term PEHEs) for a single station is generally low, so its change with duration also shows a characteristic of decreasing fluctuations. As shown in the figure, the frequency of long-term PEHEs in the YRV and SC is significantly higher than that of NC and HHV. There are noticeable regional differences in the frequency of PEHEs in eastern China. Short-term PEHEs occur mainly in the north, and PEHEs in the south are more persistent. The peaks of the frequency of the long-term PEHEs in the four regions correspond to different durations (7 days (NC), 9 days (HHV), 9 days (YRV), and 10 days (SC)). The lower the local latitude, the higher the duration of the frequency corresponding to the peak and the stronger the persistence.

Pfleiderer and Coumou (2018) pointed out that global warming has increased the EH of summer in the mid-latitudes of the Northern Hemisphere. From the late 1990s to the early 21st century, North China was controlled by a ridge of continental high pressure and the northwestern boundary of the Western Pacific subtropical high (WEI and SUN 2007). Their effect significantly increased the PEHE persistence in North China in July during this period. However, in the 2000s, the frequency of PEHEs in North China was the lowest, which may be related to the stable temperature increase caused by the PDO phase adjustment during this period (DU et al. 2018).

In the 2010s, especially in typical high-temperature years, the circulation system of the West Pacific subtropical high was significantly enhanced (Peng et al. 2016). Due to the feedback of the West Pacific subtropical high, the frequency of long-term PEHEs in the summer of 2010 increased rapidly in the south, which explains the slight decrease in the frequency of short-term PEHE events compared to the 2000s. At the same time, this illustrates the impact of global warming on long-term PEHE events in southern China more obviously. However, the frequency and sustained intensity of long-term PEHEs in the YRV are significantly stronger than in SC at lower latitudes, especially the frequency of PEHEs that last for more than 10 days. This may be related to the summer drought resulting from an anomalous geopotential height (Sun et al. 2011).

To further analyse the interdecadal changes and regional differences in summer PEHEs in eastern China, Fig. 4 shows the interannual changes in the frequency of short-term and long-term PEHEs of each station in regions of eastern China and their nine-year moving average.

From the 1960s to the 2000s, except for the long-term PEHE events in NC (Fig. 4e), the frequency of single-station PEHEs in the four regions of eastern China all showed the characteristics of interdecadal changes that first decreased and then increased, especially in the Huanghuai region. After the 1960s, the frequency of short-term PEHEs decreased significantly. Since the late 1970s, the frequency of PEHEs in

all regions of eastern China has undergone a significant interdecadal transition. The interdecadal transition in NC (Fig. 4a) occurred in the late 1980s, that of the HHV (Fig. 4b) and YRV (Fig. 4c) in the mid-1980s, and that of SC (Fig. 4d) in the early 1970s. The lower the latitude, the earlier the turning point.

In the late 1990s and early 2000s, the frequency of PEHE events in NC increased significantly. In the 2010s, the frequency of short-term PEHEs decreased in the YRV and SC, while the frequency of long-term PEHEs increased.

4. Intraseasonal Characteristics Of Pehes

4.1 Intraseasonal differences in PEHE persistence in summer

Previous studies have shown that there are obvious intraseasonal changes in the temporal and spatial distributions of EHEs in summer in eastern China and there are also obvious regional differences in interdecadal changes in eastern China (Qiao et al. 2018). To explore the intraseasonal variation and interdecadal variation of PEHEs in eastern China, the average monthly duration-frequency curve of EHEs per station in each decade in the four regions of eastern China is shown in Fig. 5.

There were obvious regional differences in the timing of PEHEs in eastern China. From June to August, short-term PEHEs occurred in NC (Fig. 5a) and HHV (Fig. 5b), but they were mainly concentrated in June and July. The frequency of long-term PEHEs was low, mainly concentrated in June and July. PEHEs in the YRV (Fig. 5c) and SC (Fig. 5d) were concentrated in July and August.

The variations in the frequency of persistent extreme high temperature in the four regions of eastern China with duration are similar to the exponential decay changes in the traditional summer. The exponential decay trend of PEHE frequency with duration is less affected by intraseasonal changes. The frequency of PEHEs in the four regions dropped rapidly within the range of short-term PEHEs. Simultaneously, the frequency of PEHEs (long-term PEHEs) for more than 7 days showed a decrease in fluctuations.

Although the frequency changes over time are similar, in northern regions, especially in NC, the frequency and persistence of PEHEs in July and August are significantly more robust in response to global warming than in June. Since the 1990s, the frequency of the long-term PEHEs in midsummer in NC is at least three times that of previous decades. Not only has the frequency of PEHEs increased significantly, but its sustainability has been considerably enhanced.

4.2 Intraseasonal differences in interdecadal changes in PEHEs

To further explore the interannual variation of PEHEs in various regions, the nine-year moving average curve and linear trend of the monthly short-term and long-term PEHE frequency in the four regions of

eastern China from 1961 to 2018 are shown in Fig. 6. Since the acceleration of global warming in the 1990s, the intraseasonal distribution of PEHE frequency in NC and HHV in eastern China has changed significantly. The occurrence time of PEHEs gradually changed from June and July to the whole summer, and the trend of different months also appeared to be different.

From the 1960s to the 1990s, variations in the frequency of short-term PEHEs from June to July in NC (Fig. 6a & 6g) and HHV (Fig. 6b & 6h) were consistent with the trend of the traditional summer (Fig. 4). In August of the late 1990s, there was a significant increase in the frequency of short-term PEHEs in the NC and HHV. In the 2010s especially, the frequency of short-term and long-term PEHEs in some years approached or even exceeded the frequency of PEHE in June. Before the 2010s, the trend of the short-term PEHE 9-year moving average curve changes in June and July in NC and HHV was the same. However, since the beginning of the 21st century, the trend in the frequency between June and July has also appeared to be different, and the correlation between the trend in July and August is higher than the correlation between June and July. Since global warming, the feedback mechanism within the season has undergone certain changes.

PEHEs in the YRV (Fig. 6c) and SC (Fig. 6d) were concentrated in July and August. During this period, the system affecting the two regions was mainly the western Pacific subtropical high (Yuan et al. 2018). Short-term PEHEs have a higher frequency and shorter duration, and the possibility of process interruption is relatively small. Therefore, the nine-year moving average of the short-term PEHE frequency over time in the two regions is basically consistent with the traditional summer PEHEs (Fig. 4c & 4d), and differences between the trend of frequency in July and August is relatively small. However, the nine-year moving average of the long-term PEHE frequency in July and August in the YRV (Fig. 6g) was quite different in the period from the late 1980s to the early 1990s and the period of 2000s. This is consistent with the statistical analysis of Shi et al. (2009) in the typical years with more high-temperature days in July in East China from 1960 to 2005. In these two periods, the number of typical years with more high-temperature days in July accounted for ten high temperatures, i.e., 70% of a typical year (1988, 1990, 1992, 1994, 2001, 2003, 2004). At the same time, August accounted for only 10% (2003) in this period (Shi et al. 2009), so the long-term PEHEs in the YRV have a large intraseasonal difference. This result may be related to the difference in the number of landing typhoons during the high-temperature period in East China. In July, a typical year with more high-temperature days, the average number of typhoons landing in East China is lower. Therefore, the continuous high-temperature processes in these two periods are not easily interrupted by the impact of precipitation caused by typhoons, and long-term PEHEs are more likely to occur.

In addition, since global warming, there are apparent intraseasonal differences in the regions where the frequency of short-term PEHEs has increased significantly in eastern China. The region with the most significant increase in short-term PEHEs in June was NC, compared with July in the HHV, and August in YRV (all passed the 95% significance test). The region with the most significant increase in the long-term PEHE frequency in July and August was the YRV (both values passed the 95% significance test).

4.3 Intraseasonal spatial distributions of PEHEs

Figures 7 and 8 show the average duration of PEHEs in June, July, and August, which lasted more than 3 days (all-PEHEs) and 7 days (long-term PEHEs), respectively. The interdecadal trends of the average duration of PEHEs in the same month are the same, while the spatial distributions are different.

In June (Fig. 7a), the area of the average duration of all PEHEs is distributed in NC and HHV, consistent with the above conclusion. The area of long-term PEHEs is mainly scattered in northern regions. Affected by plum rain, there are relatively fewer EHEs in the YRV in June. It is worth noting that the PEHE centres exceeding 3 days in the HHV are mainly located in inland areas, showing the opposite distribution from July, which is supposed to be affected by the northern region of the plum rain (Tao et al. 1958).

In July (Fig. 7b), the scope and persistence of PEHEs increased significantly in NC. The high-value centre of the duration of all PEHEs in HHV also moved from inland to coastal areas. The incidence of PEHEs in the YRV and SC has increased rapidly, and the persistence is far beyond that in northern China. The most persistent PEHEs in eastern China are roughly located in the YRV. In August (Fig. 7c), the area where PEHEs occurred decreased, but since the 2010s, the persistence of PEHEs in the YRV and HHV has increased obviously (Fig. 8c), even exceeding that in July (Fig. 8b).

4.4 Comparisons of composite circulation anomalies for different regions

In the northern-hemispheric mid-latitudes, several extreme events have been linked to anomalous atmospheric circulation patterns favoring the persistence of local weather conditions (Qiao et al. 2011, Pfliegerer and Coumou 2018). The circulation associated with EHEs in eastern China typically shows an anomalous anticyclone that enhances temperature through adiabatic heating (Sun et al. 2011, Chen & Lu, 2015). In order to analyse the likely mechanism which results in the differences in the PEHE in eastern China, the circulation anomalies associated with EH are systematically compared. Figure 9 and Fig. 10 show the average composite of 500hPa and 850hPa geopotential height anomaly in eastern China, and 850hPa (e, f) meridional wind anomaly of strong-persistence years since the 1990s in SC and YRV. There is an anomalous anticyclone over the region in the middle and low troposphere in the four regions, respectively.

In June, there is a significant anticyclone over the NC (Fig. 9a & 9b) in both the middle and lower troposphere, and the centre are both located in the north of 40°N. The circulation anomalies in HHV (Fig. 9c & 9d) are similar to NC, so the nine-year moving average of the frequency of the PEHE in NC and HHV is likely in June. Figure 10a and 10b shows the composite anomalies of the strong-persistence years in YRV in July. There is also a significant anticyclone in the middle and lower troposphere, but located in the east of the region. Meanwhile, the centre of composite anticyclone anomalies in SC in July is in the southeast of the region (Fig. 10c & 10d). The differences in the position of the anticyclone anomalies between June and July resulting in the intraseasonal variations of the PEHE in eastern China. In addition, in southern China, there is a positive meridional wind anomaly in the lower troposphere (Fig. 10e & 10f), which is also an important reason for the difference between PEHE in southern and northern China (Huang et al. 1993, Sun et al. 2011, Qiao et al. 2018).

5. Variations Of The Persistence In Pehes Under Global Warming

The above analysis has shown the regional differences in the frequency of PEHEs in eastern China. Since global warming, the intraseasonal variation in PEHEs in the HHV has differed significantly from that in the previous period. The persistence of PEHEs in the YRV and SC has increased. Therefore, we analysed the persistence of PEHEs in the two periods before and after global warming (P1: 1961–1990; P2: 1991–2018).

Figure 10 shows the probability density distribution of the average duration of PEHEs in the four regions of eastern China during the period 1961–2018 (P), P1, and P2. In period P2, the maximum boundary values of HHV, YRV, and SC reached 14, 14, and 14.5 days (increased by 4.7 days (HHV), 3 days (YRV) and 2.5 days (SC), respectively, compared with P1), showing that since global warming, the persistence of PEHEs in the three regions has increased.

In addition, in NC (Fig. 11a) and HHV (Fig. 11b), the probability distribution of P2 on the right side (larger value) is higher than P1, indicating that the average duration of PEHEs in these regions has increased (Zhan et al. 2020). In other words, in the HHV, since global warming, the persistence of PEHEs has increased, and the average intensity of the PEHEs has increased at the same time.

6. Conclusion And Discussion

Using the daily maximum temperature data of 759 stations in eastern China from May to September from 1961 to 2018 and the data sets of the NCEP-NCAR Reanalysis, this paper analyses the temporal and spatial characteristics and regional characteristics of PEHEs in NC, HHV, YRV, and SC. We distinguished duration in this study and discussed the persistence of the EHE. And the PEHE was discussed month by month instead of traditional summer to study the intraseasonal variations. The conclusions are as follows:

The frequency of PEHEs in eastern China decays exponentially with time. In terms of spatial distribution, there is a regional difference in the duration and intraseasonal differences in the occurrence time. The northern site is dominated by multi-frequency, short-duration EHEs, compared to the opposite in the south. PEHEs in NC and HHV mainly occur from June to July, while in the south, they mainly occur from July to August.

Since the 1990s, the response of PEHEs in northern regions to the global warming has become more apparent with more frequency, stronger persistence and obvious intraseasonal differences. The frequency of PEHEs increases in July and August, shows an opposite linear trend in June. The interdecadal trend in PEHEs also showed apparent differences. Since the 2000s, the frequency and persistence of PEHEs has increased significantly in the YRV and SC, especially the long-term PEHEs since 2010s. The differences in the position of the anticyclone anomalies in both the middle and lower troposphere resulting in the intraseasonal variations of the PEHE in eastern China.

This study is mainly based on the PEHEs of a single site. The average annual situation and each decade are represented by the site. The current results show that interdecadal and variation of the PEHE and circulation associated with differences of the PEHE are consistent with previous studies in EHE in eastern China. In future work, it is necessary to conduct a more in-depth exploration of the characteristics and mechanisms of the large-scale variations of PEHEs since global warming on the basis of this work. The statistical result can then be used in combination with a dynamic forecast and can be applied to seasonal prediction.

Declarations

Conflict of Interest

The authors declare that they have no known competing financial interests or personal relationships that could have appeared to influence the work reported in this paper.

Consent to participate

(Not applicable)

Consent for publication

(Not applicable)

Ethics approval (Not applicable)

Funding Statement

This study was jointly supported by the National Key Research and Development Program of China [grant numbers 2017YFC1502303 and 2018YFA0606301]; the National Natural Science Foundation of China (NSFC) [grant number 42075017 and 41875093].

Author's contribution

All authors contributed to the study conception and design.

Conceptualization: Naihui Zang, Junhu Zhao, Pengcheng Yan and Guolin Feng; Methodology: Naihui Zang, Junhu Zhao, Pengcheng Yan; Formal analysis and investigation: Naihui Zang, Han Zhang, Shankai Tang; Writing: Naihui Zang.

All authors commented on previous versions of the manuscript. All authors read and approved the final manuscript.

Availability of data and material

The NCEP-NCAR Reanalysis datasets generated during and/or analysed during the current study are available from the corresponding author on reasonable request. The observed daily surface air temperature data for 2,374 stations that are available from the National Weather Information Center of the China Meteorological Administration.

Code availability

The code analysed during the current study are available from the corresponding author on reasonable request.

References

1. Allen MR, Dube OP, Solecki W, Aragón-Durand F (2018) Special Report: Global warming of 1.5°C. IPCC
2. Chen RD, Lu RY (2015) Comparisons of the Circulation Anomalies Associated with Extreme Heat in Different Regions of Eastern. China *J Climate* 28:5830–5844. DOI:10.1175/JCLI-D-14-00818.1
3. Ding T, Qian WH, Yan ZW (2010) Changes in hot days and heat waves in China during 1961–2007. *Int J Climatol* 30:1452–1462. doi:10.1002/joc.1989
4. Dole R et al (2011) Was there a basis for anticipating the 2010 Russian heat wave? *Geophys Res Lett* 38 doi:10.1029/2010gl046582
5. DU Q, ZHANG M, WANG S, CHE C, QIU X, MA Z (2018) Changes in air temperature of China in response to global warming hiatus. *J Geog Sci* 73:1748–1764. doi:10.11821/dlxb201809011
6. Fischer EM, Knutti R (2015) Anthropogenic contribution to global occurrence of heavy-precipitation and high-temperature extremes. *Nat Clim Change* 5:560–564. doi:10.1038/nclimate2617
7. Hoerling M et al (2013) Anatomy of an Extreme. Event *J Climate* 26:2811–2832. doi:10.1175/Jcli-D-12-00270.1
8. Hong HX, Sun JQ, Wang HJ (2020) Interdecadal variation in the frequency of extreme hot events in Northeast China and the possible mechanism *Atmospheric Research* 244 doi:ARTN 105065 1016/j.atmosres.2020.105065
9. Huang J, Yi Y, Wang S, Chou J (1993) An analogue-dynamical long-range numerical weather prediction system incorporating historical evolution *Quarterly. Journal of the Royal Meteorological Society* 119:547–565. doi:10.1002/qj.49711951111
10. Jia J, Hu Z (2017) Spatial and Temporal Features and Trend of Different Level Heat Waves Over China *Advances in Earth Science*. (in Chinese) 32:546–559. doi:10.11867/j.issn.1001-8166.2017.05.0546

11. Kalnay E et al (1996) The NCEP/NCAR 40-year reanalysis project. *B. Am Meteorol Soc* 77:437–471
doi:10.1175/1520-0477
12. Karmalkar AV, Bradley RS (2017) Consequences of Global Warming of 1.5 degrees C and 2 degrees C for Regional Temperature and Precipitation Changes in the Contiguous United States. *Plos One* 12
doi:10.1371/journal.pone.0168697
13. LU C, SUN Y, CHRISTIDIS N, STOTT PA (2020) Contribution of Global Warming and Atmospheric Circulation to the Hottest Spring in Eastern China in 2018. *Adv Atmos Sci* 33:1285–1294.
doi:10.1007/s00376-020-0088-5
14. Lu CH, Sun Y, Zhang XB (2018) Multimodel detection and attribution of changes in warm and cold spell durations. *Environ Res Lett* 13 doi:ARTN 07401310.1088/1748-9326/aacb3e
15. Luterbacher J, Dietrich D, Xoplaki E, Grosjean M, Wanner H (2004) European seasonal and annual temperature variability, trends, and extremes since 1500. *Science* 303:1499–1503.
doi:10.1126/science.1093877
16. Meehl GA, Tebaldi C (2004) More intense, more frequent, and longer lasting heat waves in the 21. st century. *Science* 305:994–997 doi. DOI 10.1126/science.1098704
17. Min SK, Zhang XB, Zwiers F, Shiogama H, Tung YS, Wehner M (2013) Multimodel Detection and Attribution of Extreme Temperature. *Changes J Climate* 26:7430–7451. doi:10.1175/Jcli-D-12-00551.1
18. Peng J, Liu G, Sun S (2016) An Analysis on the Formation of the Heat Wave in Southern China and Its Relation to the Anomalous Western Pacific Subtropical High in the Summer of 2013. *Chinese Journal of Atmospheric Sciences (in Chinese)* 40:897_906
19. Peng J, Zhang Q, Cholaw B (2007) On the Characteristics and Possible Causes of A Severe Drought and Heat Wave in the Sichuan-Chongqing Region in 2006. *Climatic and Environmental Research. (in Chinese)* 12:464–474. doi:10.3969/j.issn.1006-9585.2007.03.026
20. Pfleiderer P, Coumou D (2018) Quantification of temperature persistence over the Northern Hemisphere land-area. *Climate Dynamic* 51:627–637. doi:10.1007/s00382-017-3945-x
21. Qin D, Zhang J, Shan C (2015) China National Assessment Report on Risk Management and Adaptation of Climate Extremes and Disasters. Science Press
22. Qiao SB, Gong ZQ, Feng GL, Qian ZH (2015) Relationship between cold winters over Northern Asia and the subsequent hot summers over mid-lower reaches of the Yangtze River valley under global warming. *Atmos Sci Lett* 16:479–484
23. Qiao SB et al (2018) Enhancement of the relationship between the winter Arctic oscillation and the following summer circulation anomalies over central East Asia since the early 1990. *s Clim Dynam* 50:3485–3503. doi:10.1007/s00382-017-3818-3
24. Ren LW, Zhou TJ, Zhang WX (2020) Attribution of the record-breaking heat event over Northeast Asia in summer 2018: the role of circulation. *Environ Res Lett* 15 doi:ARTN 054018 1088/1748-9326/ab8032

25. Robine J-M, Cheung SLK, Roy SL, Oyen HV, Griffiths C, Michel J-P, Herrmann FoR (2008) Death toll exceeded 70,000 in Europe during the summer of 2003. *Comptes rendus biologiques* 331:171–178. doi:10.1016/j.crvi.2007.12.001
26. Shi J, Ding YH, Cui LL (2009) Climatic characteristics of extreme maximum temperature in East China and its causes Chinese. *J Atmos Sci* 33:347–358
27. Stocker T (2014) *Climate change 2013: the physical science basis : Working Group I contribution to the Fifth assessment report of the Intergovernmental Panel on Climate Change*. Cambridge University Press, New York
28. Sun JQ, Wang HJ, Yuan W (2011) Decadal Variability of the Extreme Hot Event in China and Its Association with Atmospheric Circulations *Climatic and Environmental Research*. (in Chinese) 16:199–208
29. Sun Y, Zhang XB, Ren GY, Zwiers FW, Hu T (2016) Contribution of urbanization to warming in China. *Nat Clim Change* 6:706–709. doi:10.1038/nclimate2956
30. Sun Y et al (2014) Rapid increase in the risk of extreme summer heat in Eastern China. *Nat Clim Change* 4:1082–1085. doi:10.1038/NCLIMATE2410
31. Tang SK, Qiao SB, Feng TC, Jia ZK, Zang NH, Feng GL (2020) Predictability of the mid-summer surface air temperature over the Yangtze River valley in the National Centers for Environmental Prediction Climate Forecast System *Int J Climatol* 1 doi:10.1002/joc.6670
32. Tao SY, Zhao YJ, Chen XM (1958) The Relationship Between May-Yu in Far East And The Behaviour of Circulation over Asia *Acta Meteorologica Sinica*. (in Chinese) 29:119–134
33. Vincent LA, Mekis E (2006) Changes in daily and extreme temperature and precipitation indices for Canada over the twentieth century. *Atmos Ocean* 44:177–193. doi:10.3137/ao.440205
34. Wang G, Ye D, Zhang Y, Huang D, Hou W (2018) Characteristics and abnormal atmospheric circulation of regional high temperature process in 2017 over China *Adv. Atmos Sci* 14:341–349. doi:10.12006/j.issn.1673-1719.2018.008
35. Wang J, Chen Y, Tett SFB, Yan Z, Zhai P, Feng J, Xia J (2020) Anthropogenically-driven increases in the risks of summertime compound hot extremes *NATURE COMMUNICATIONS* 11 doi:10.1038/s41467-019-14233-8
36. Wang JM et al (2021) Changing Lengths of the Four Seasons by Global Warming *Geophys Res Lett* 48 doi:10.1029/2020GL091753
37. Wang Y, Ren F, Yan F (2013) Study on Temporal and Spatial Variations of Regional Continual High Temperature Event in China *Scientia Geographica Sinica* (in Chinese) 33 doi:10.13249/j.cnki.sgs.2013.03.014
38. WEI J, SUN J (2007) The Analysis of Summer Heat Wave and Sultry Weather in North China (in Chinese) *Climatic and Environmental Research*. (in Chinese) 12:453–463. doi:10.3969/j.issn.1006-9585.2007.03.025
39. XU K, Lu R, MAO J, CHEN R (2019) Circulation anomalies in the mid–high latitudes responsible for the extremely hot summer of 2018 over northeast Asia *ATMOSPHERIC AND OCEANIC. SCIENCE*

40. Yang H, Feng G (2016) Diagnostic Analyses of Characteristics and Causes of Regional and Persistent High Temperature Event in China Plateau Meteorology (in Chinese) 35
doi:10.7522/j.issn.1000-0534.2014.00130
41. Ye D, Yin J, Chen Z, Zheng Y, Wu R (2013) Spatiotemporal Change Characteristics of Summer Heatwaves in China in 1961–2010 Advances in Climate Change. Research(in Chinese) 9:015–020
42. Yuan Y, Ding T, Gao H, Li W (2018) Major Modes of Midsummer Air Temperature in Southern China and Their Relationship with Sea Surface Temperature Anomalies Chinese Journal of Atmospheric Sciences. (in Chinese) 42:1245–1262
43. Zang N, Zhao J, Yan P, Feng G (2019) Interdecadal Variations of the Temporal and Spatial Distribution of Summer Extreme Heat in. China Atmos Ocean 57:365–377.
doi:10.1080/07055900.2019.1692189
44. Zhan W, He XG, Sheffield J, Wood EF (2020) Projected Seasonal Changes in Large-Scale Global Precipitation and Temperature Extremes Based on the CMIP5. Ensemble J Climate 33:5651–5671.
doi:10.1175/Jcli-D-19-0311.1
45. Zhang QY, Wei J, Tao SY (2003) The Decadal and Interannual Variations of Drought in the Northern China and Association with the Circulations Climatic and Environmental Research. (in Chinese) 8:307–318. doi:10.3969/j.issn.1006-9585.2003.03.005
46. Zhou J, Zhi R, Li Y, Zhao J, Xiang B, Wu Y, Feng G (2020) Possible causes of the significant decrease in the number of summer days with light rain in the east of southwestern. China Atmospheric Research 236:104804. doi:10.1016/j.atmosres.2019.104804

Figures

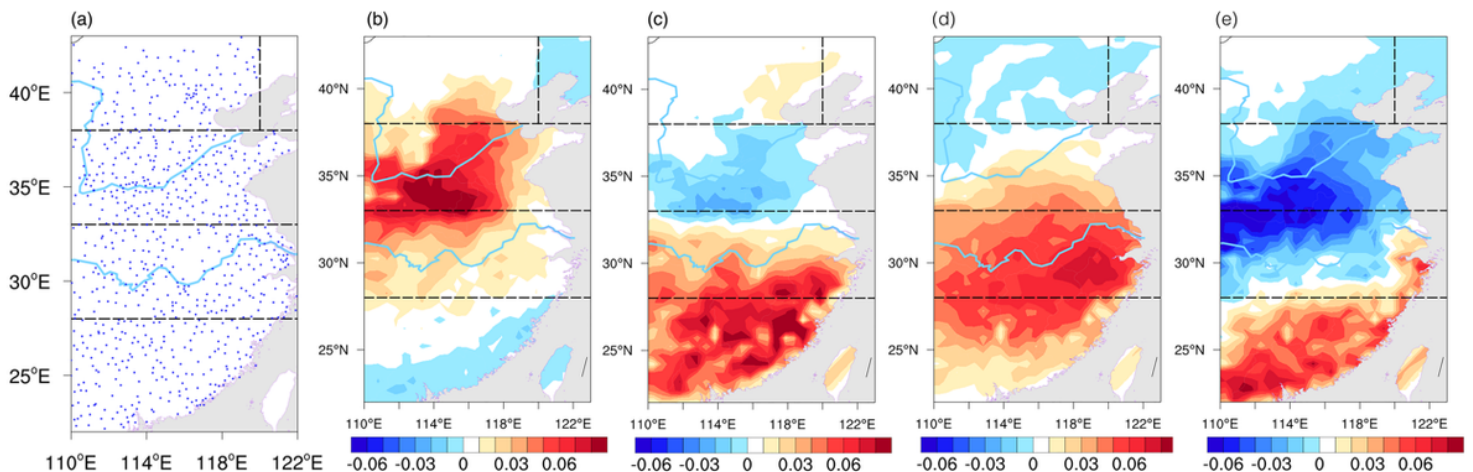


Figure 1

The spatial distribution of the 759 sites in eastern China (a), and the first two leading EOF modes of the anomaly of the number of EH days in early summer for the 1961–2018 period in eastern China: (b) EOF1 of early summer, (c) EOF2 of early summer, (d) EOF1 of midsummer, (e) EOF2 of midsummer. Note: The designations employed and the presentation of the material on this map do not imply the expression of any opinion whatsoever on the part of Research Square concerning the legal status of any country, territory, city or area or of its authorities, or concerning the delimitation of its frontiers or boundaries. This map has been provided by the authors.

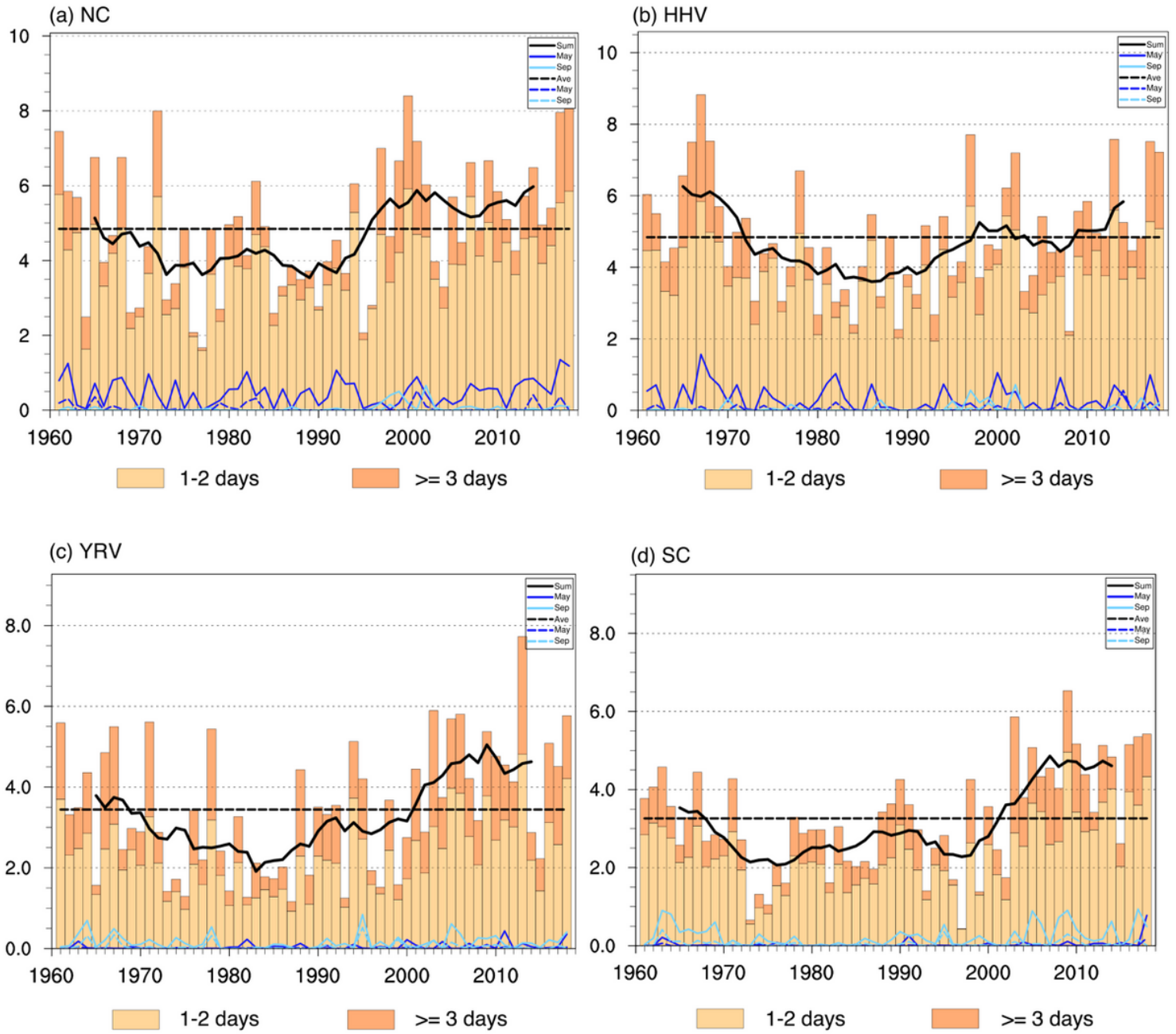


Figure 2

Interannual changes in the average number of EHEs per station in four regions in eastern China from May to September 2018. (a). NC, (b). HHV, (c). YRV, (d). SC. The light bar graph represents the number of EHEs with a duration of 1-2 days, and the dark bar graph represents the number of EHEs with a duration of 3 days or more. The black dashed line is the 58-year average, and the solid line is the nine-year moving average curve. The purple (green) solid line is the number of EHEs lasting 1-2 days in May (September), and the dashed line is the number of EHEs lasting 3 days or more.

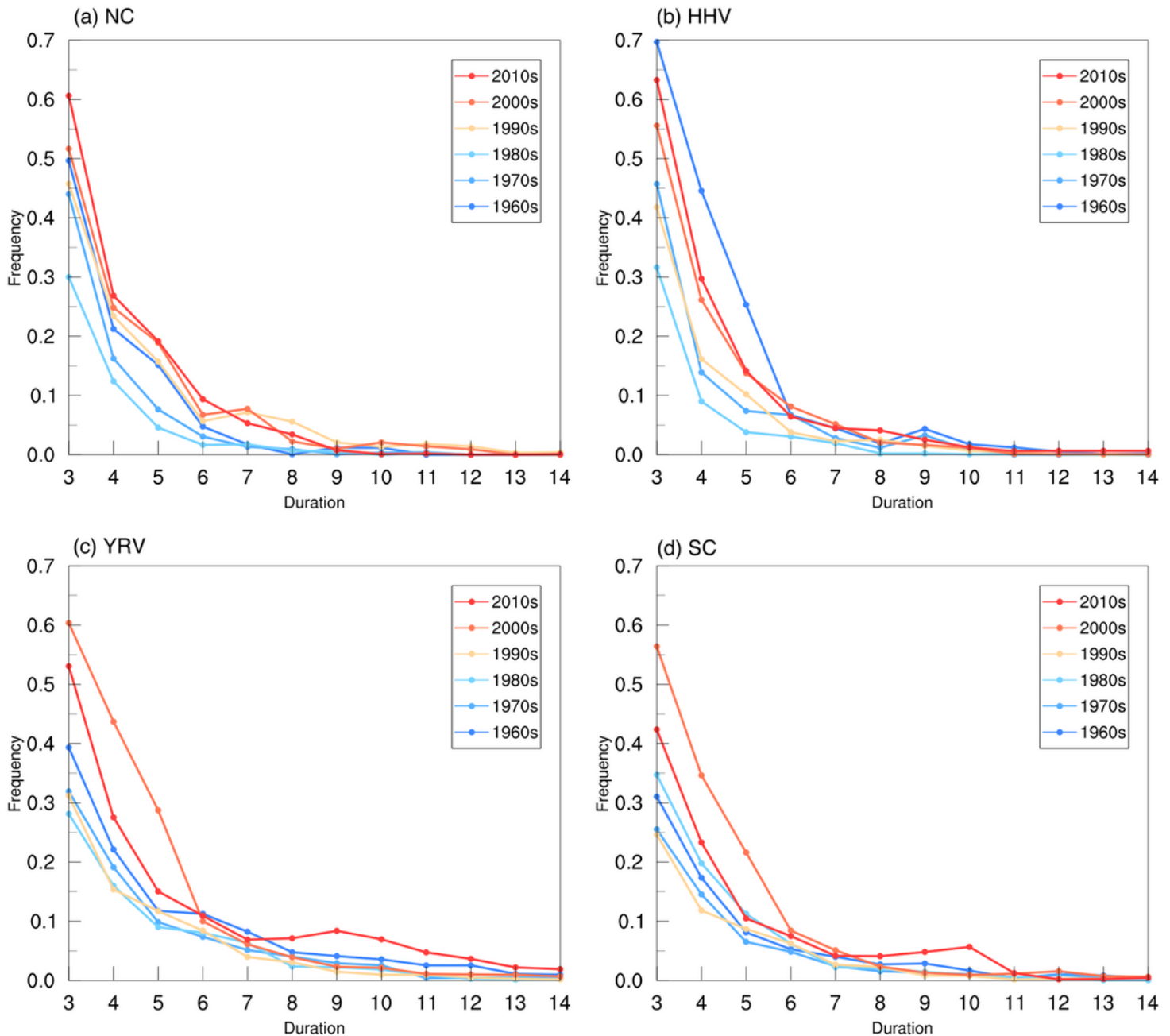


Figure 3

Different duration-frequency curves of summer PEHEs at a single station in North China from 1961 to 2018. The X-axis is the duration of PEHEs (unit: day), and the Y-axis is the average annual occurrence

frequency of a single station corresponding to each duration (data for the 2010s are 2011-2018).

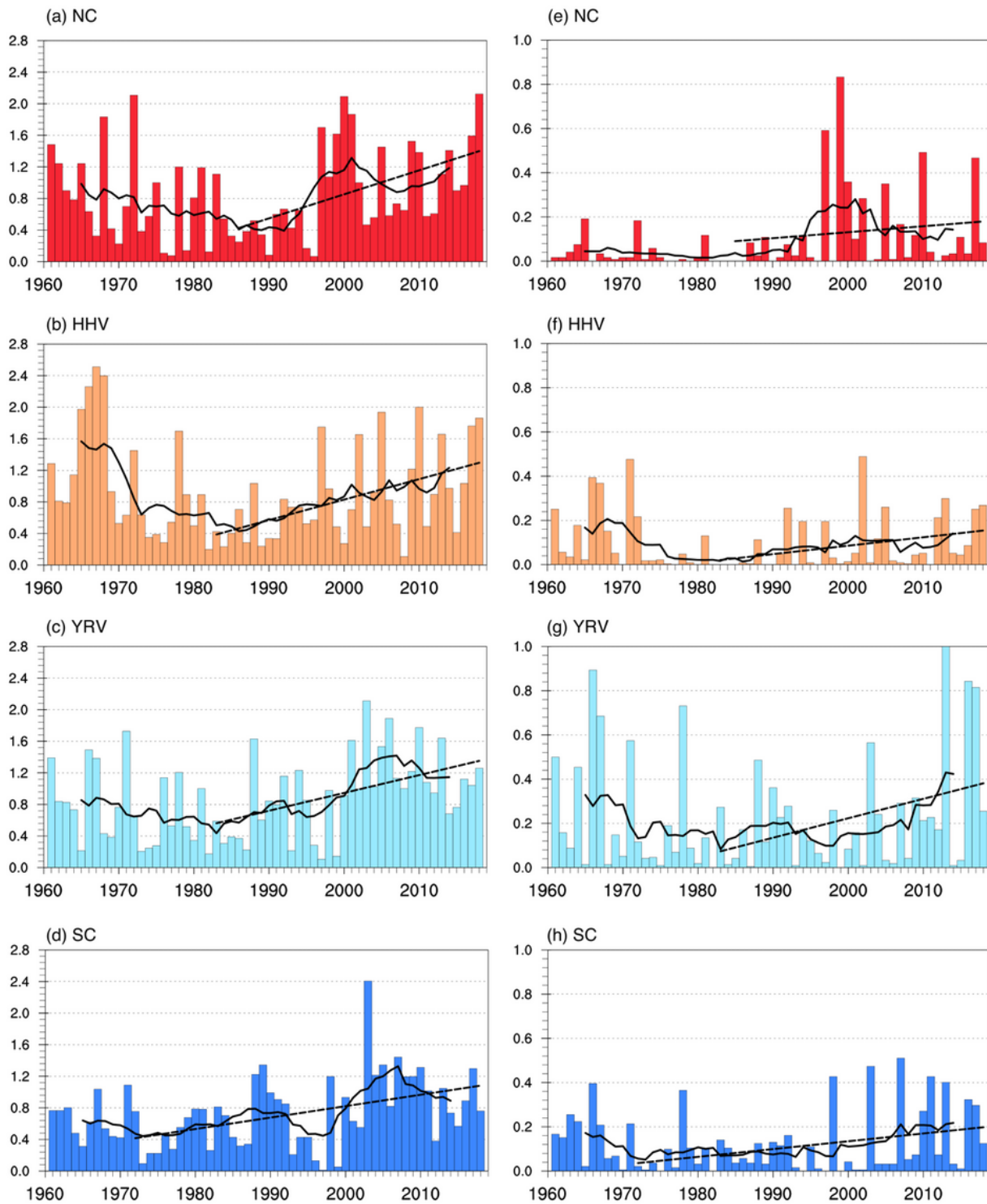


Figure 4

Frequency (histogram), linear trend (dashed line) and nine-year running mean (solid line) of short-term (a-d) and long-term (e-h) PEHEs of each station in four regions of eastern China. All the linear trend passed the 90% significance test (except for the long-term of NC).

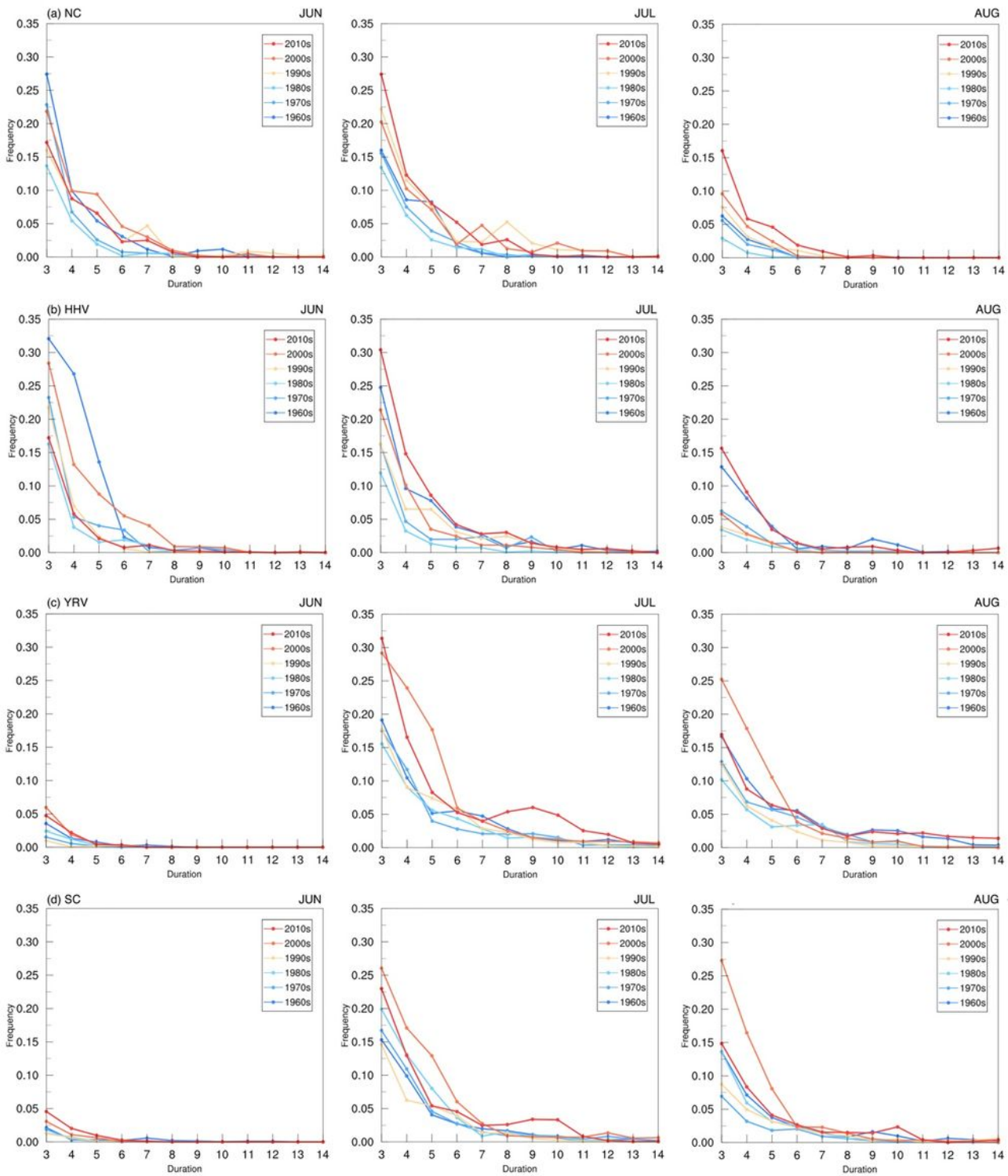


Figure 5

Monthly duration-frequency curves of summer PEHEs at a single station in eastern China of each decade from 1961 to 2018 (data for the 2010s are 2011-2018). The X-axis is the duration of PEHEs (unit: day), and the Y-axis is the average annual occurrence frequency of a single station corresponding to each duration. (a) NC, (b) HHV, (c) YRV, (d) SC.

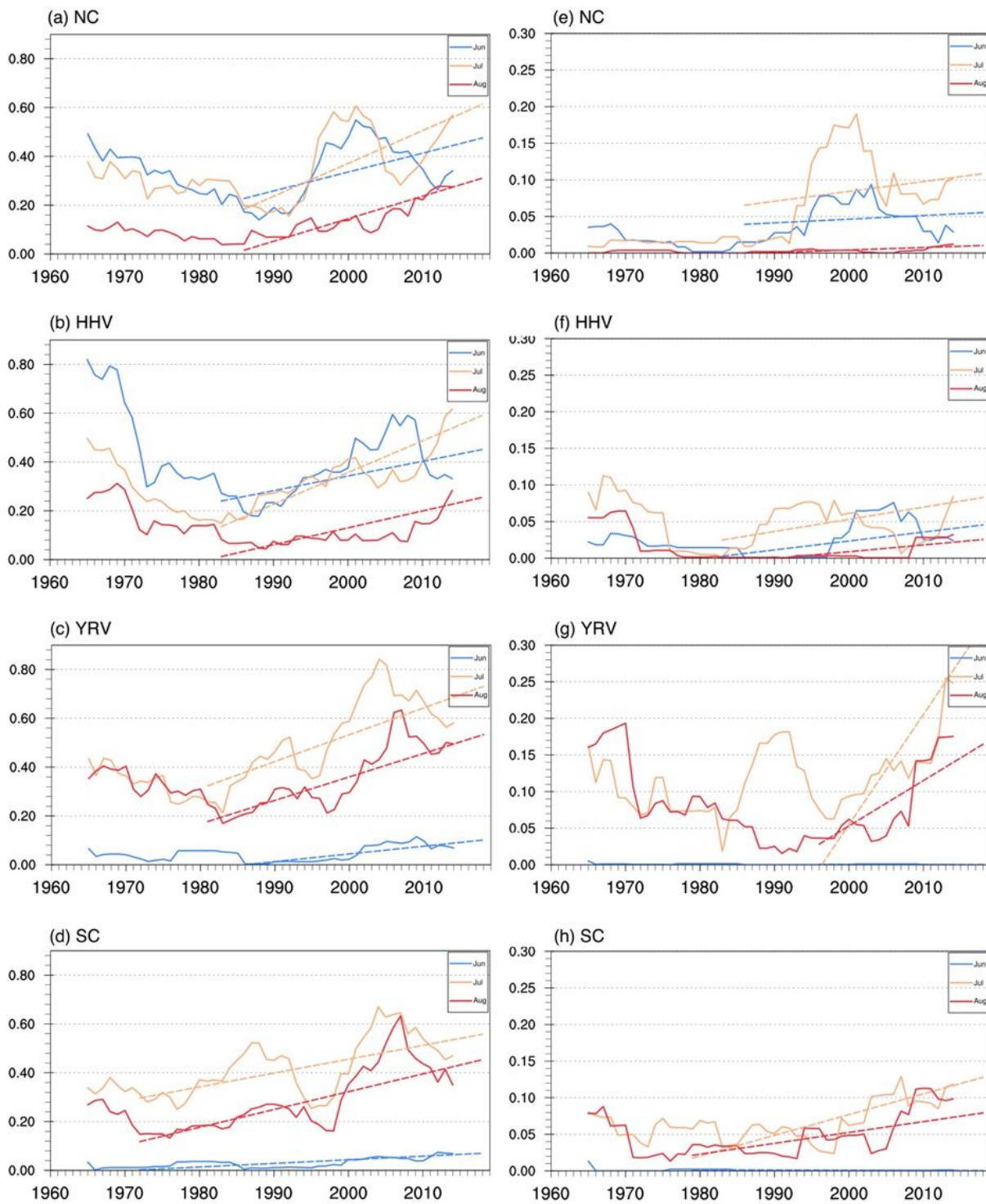


Figure 6

Nine-year moving average curve (solid line) and linear trend (dashed line) of monthly short-term (a-d) and long-term (e-h) PEHE frequency in summer in four regions of eastern China.

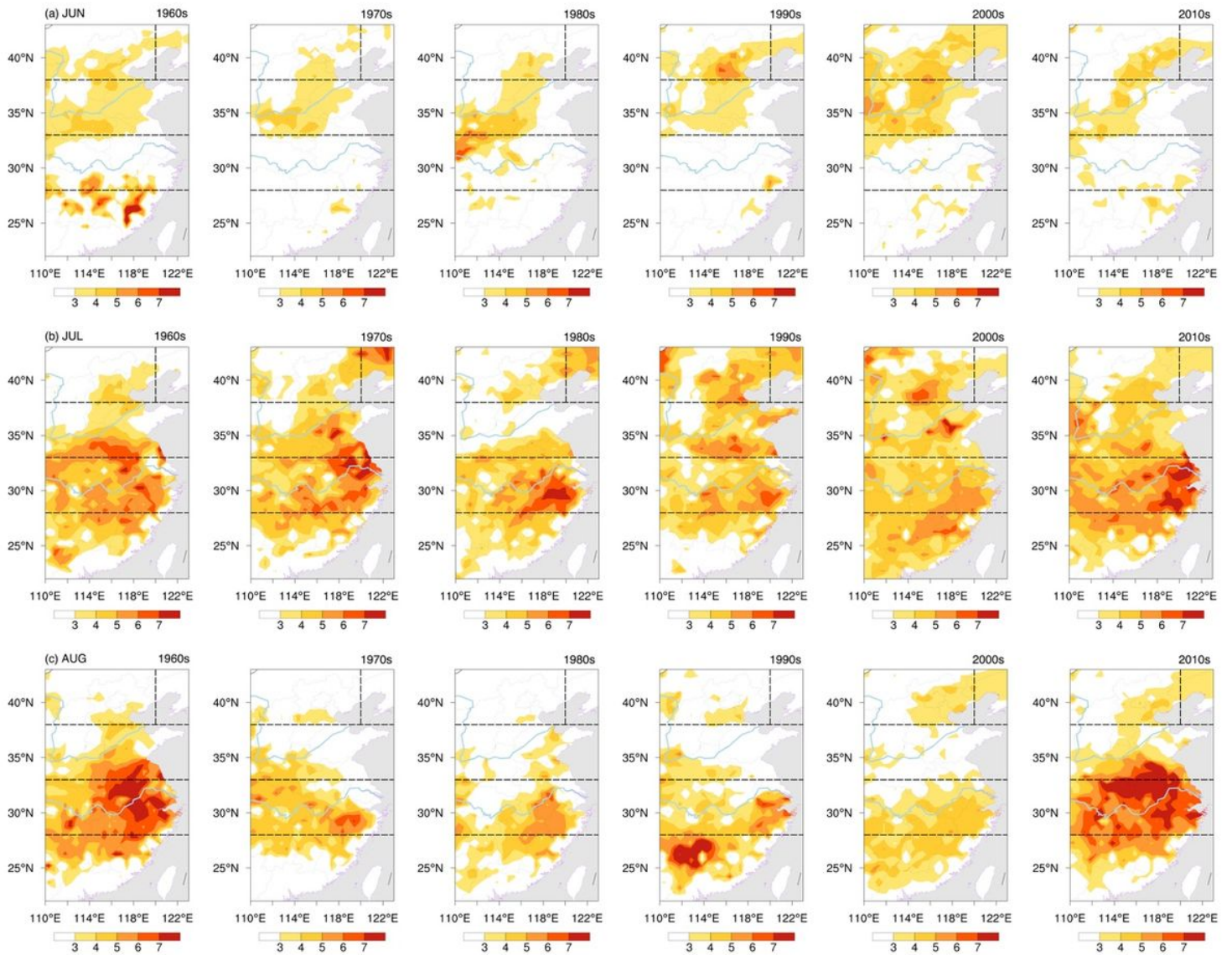


Figure 7

The average composite of 500hPa (a, b) and 850hPa (c, d) geopotential height anomaly of strong-persistence years since the 1990s in eastern China in June. (a, c) NC, (b, d) HHV. The area that at the 95% confidence level are dotted. Note: The designations employed and the presentation of the material on this map do not imply the expression of any opinion whatsoever on the part of Research Square concerning the legal status of any country, territory, city or area or of its authorities, or concerning the delimitation of its frontiers or boundaries. This map has been provided by the authors.

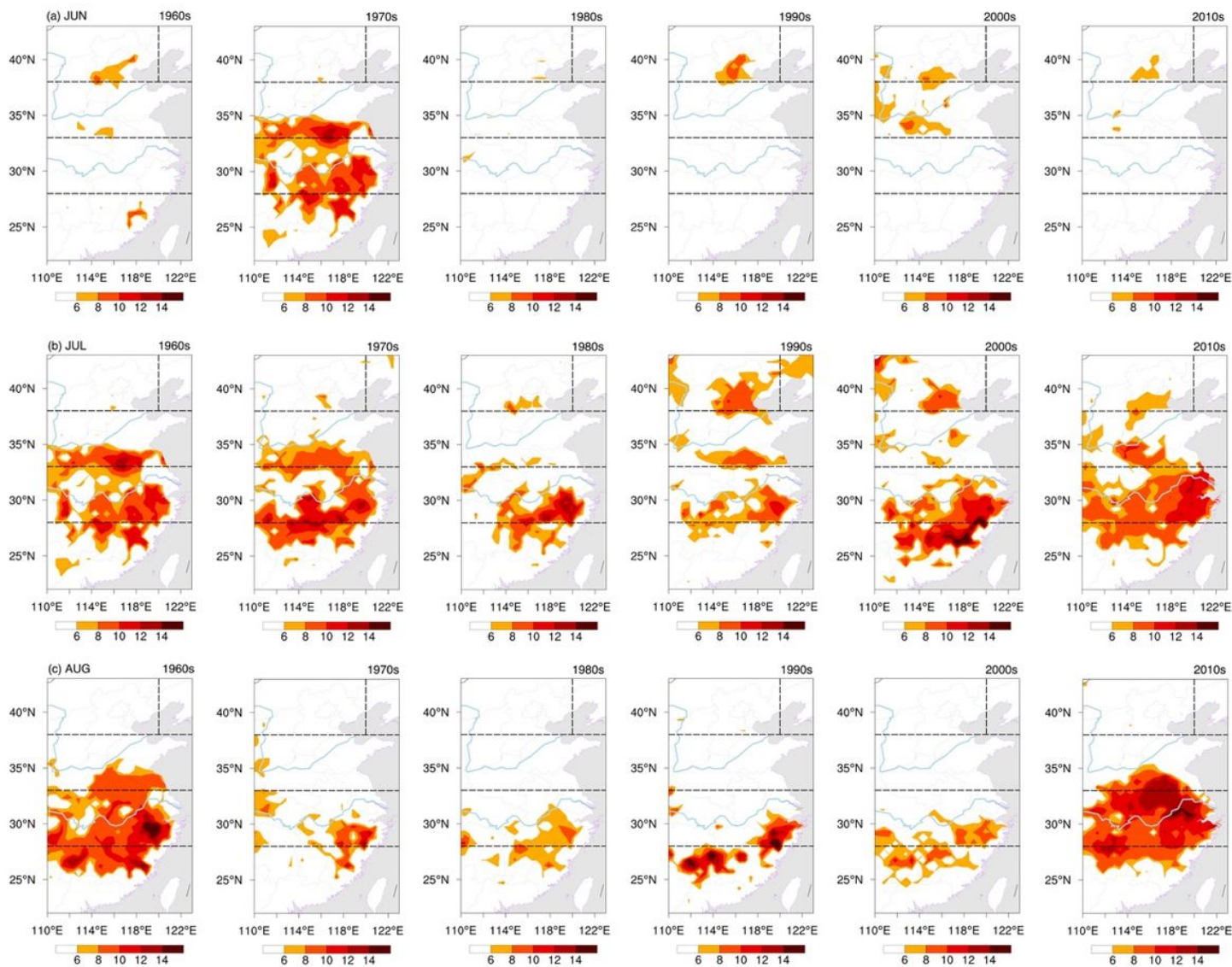


Figure 8

The same as Figure 7, but lasting 7 days or more. Note: The designations employed and the presentation of the material on this map do not imply the expression of any opinion whatsoever on the part of Research Square concerning the legal status of any country, territory, city or area or of its authorities, or concerning the delimitation of its frontiers or boundaries. This map has been provided by the authors.

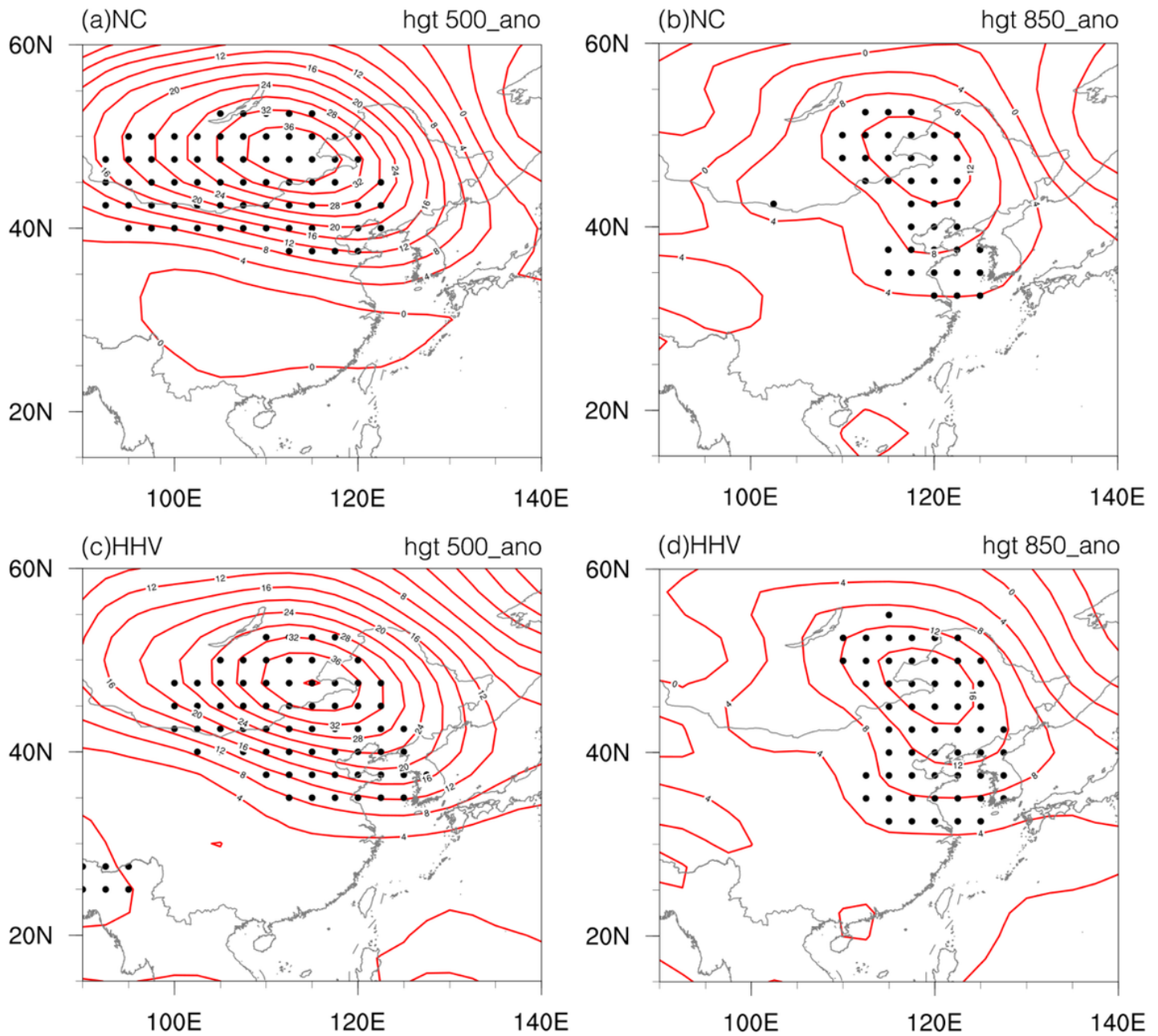


Figure 9

The average composite of 500hPa (a, b) and 850hPa (c, d) geopotential height anomaly of strong-persistence years since the 1990s in eastern China in June. (a, c) NC, (b, d) HHV. The area that at the 95% confidence level are dotted. Note: The designations employed and the presentation of the material on this map do not imply the expression of any opinion whatsoever on the part of Research Square concerning the legal status of any country, territory, city or area or of its authorities, or concerning the delimitation of its frontiers or boundaries. This map has been provided by the authors.

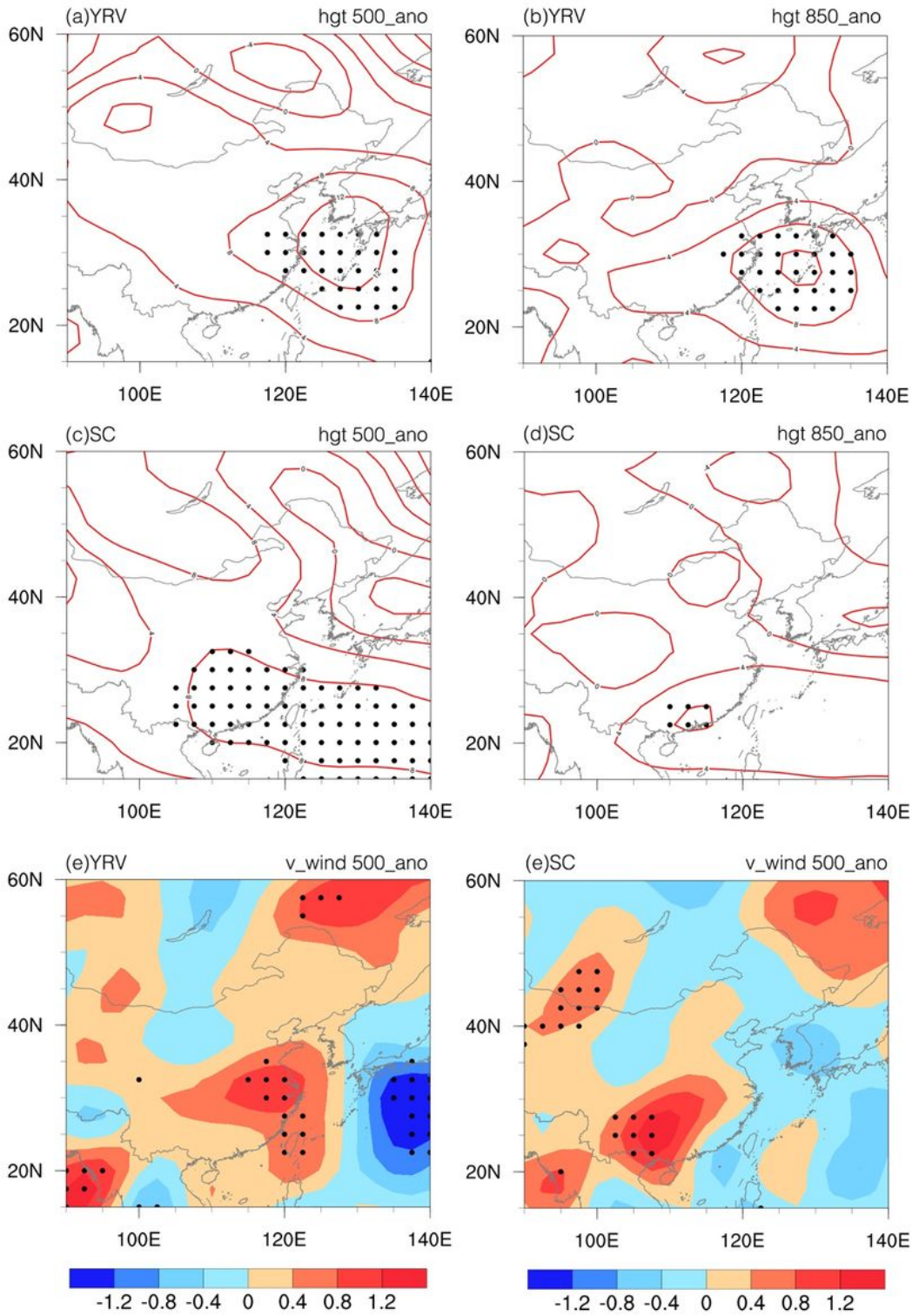


Figure 10

The average composite of 500hPa (a, b), 850hPa (c, d) geopotential height anomaly and 850hPa (e, f) meridional wind anomaly of strong-persistence years since the 1990s in eastern China in July. (a, c, e) YRV, (b, d, f) SC. The area that at the 95% confidence level are dotted. Note: The designations employed and the presentation of the material on this map do not imply the expression of any opinion whatsoever on the part of Research Square concerning the legal status of any country, territory, city or area or of its

authorities, or concerning the delimitation of its frontiers or boundaries. This map has been provided by the authors.

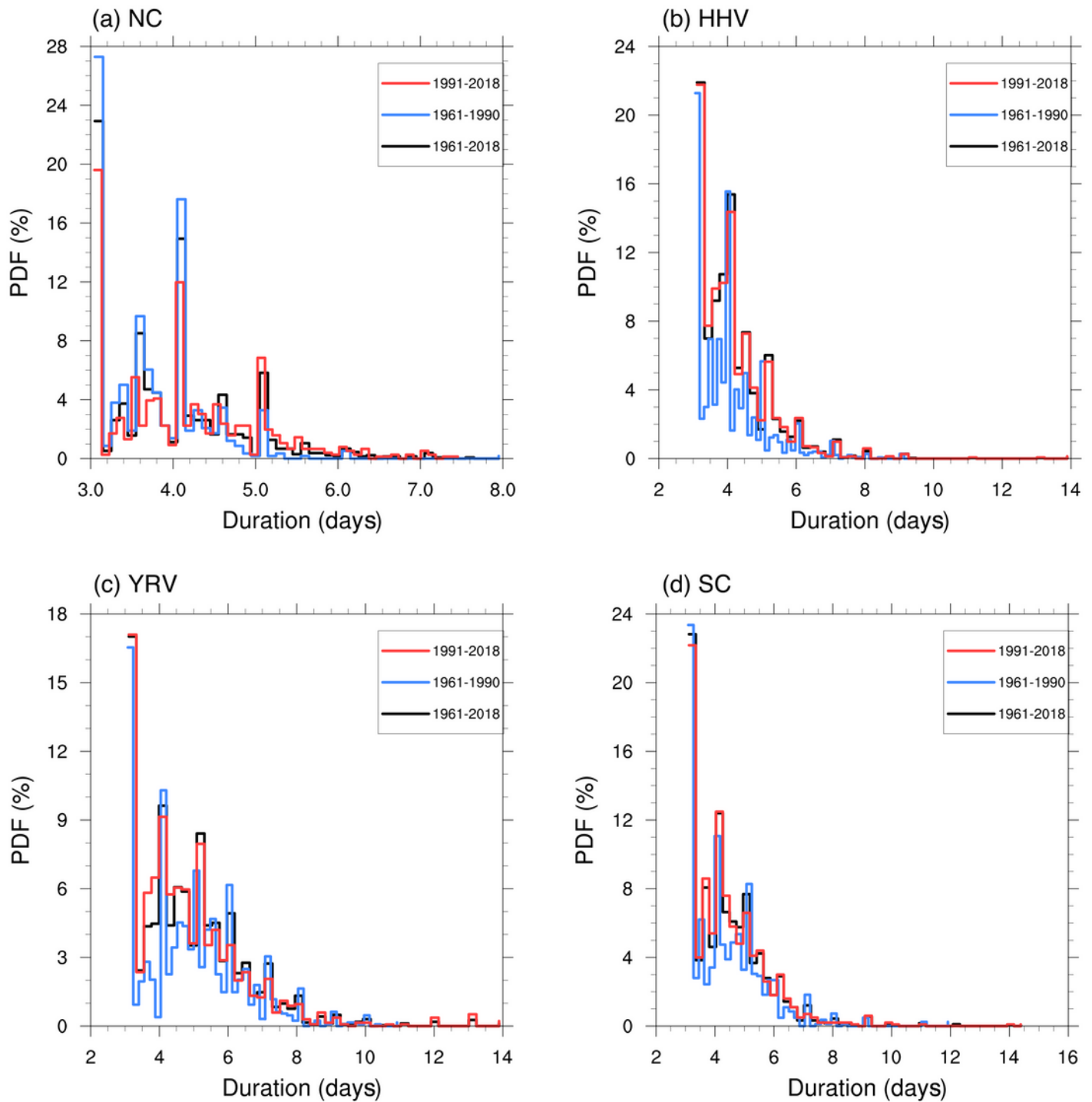


Figure 11

Probability density distribution of the average duration of PEHEs in eastern China during 1961-2018 (P) (black line), 1961-1990 (P1) (blue line), and 1991-2018 (P2) (red line). (a) NC, (b) HHV, (c) YRV, (d) SC.